

Characterization of $\text{Bi}_4\text{Ti}_3\text{O}_{12}$ powder prepared by the citrate and oxalate coprecipitation processes

Titipun Thongtem*, Somchai Thongtem

Faculty of Science, Chiang Mai University, Chiang Mai 50200, Thailand

Received 22 November 2003; received in revised form 11 December 2003; accepted 23 December 2003

Available online 8 May 2004

Abstract

Bismuth titanate ($\text{Bi}_4\text{Ti}_3\text{O}_{12}$) powder was prepared by citrate and oxalate coprecipitation of bismuth nitrate pentahydrate, $\text{Bi}(\text{NO}_3)_3 \cdot 5\text{H}_2\text{O}$ and titanium butoxide, $\text{Ti}(\text{OC}_4\text{H}_9)_4$. The intermediate products with 500–1000 °C calcination were characterized using the XRD. At low temperature, $\text{Bi}_4\text{Ti}_3\text{O}_{12}$ powder and some impurities were detected. At 1000 °C, the purified powder was obtained. At 700 °C and above, the powder underwent a phase transformation from tetragonal to orthorhombic. By using the TGA, the intermediates prepared by the citrate and oxalate coprecipitation processes were the citrate salt and the oxalate–hydroxide mixture, respectively. The FTIR analysis showed the Ti–O stretching in the 811–816 and 574–584 cm^{-1} . The morphologies shown by the SEM micrographs were consistent with the XRD patterns.
© 2004 Elsevier Ltd and Techna Group S.r.l. All rights reserved.

Keywords: $\text{Bi}_4\text{Ti}_3\text{O}_{12}$; Citrate and oxalate coprecipitation

1. Introduction

$\text{Bi}_4\text{Ti}_3\text{O}_{12}$ is classified in the Aurivillius family. It can be represented by the general formula $(\text{Bi}_2\text{O}_2)^{2-}(\text{A}_{m-1}\text{B}_m\text{O}_{3m+1})^{2+}$ in which $\text{A} = \text{Bi}$, $\text{B} = \text{Ti}$ and $m = 3$ [1–3]. It has low dielectric permittivity and a high Curie point (675 °C) [3]. At 600 °C and below, $\text{Bi}_4\text{Ti}_3\text{O}_{12}$ is the tetragonal phase and undergoes the phase transformation to orthorhombic at 750 °C [4]. It is useful for various applications such as memory storage, optical display, piezoelectric converters or pyroelectric devices over a wide range of temperatures [3,5–9]. Therefore, it is important to study the dependence of the crystal structure on the calcination process. At low temperature, $\text{Bi}_4\text{Ti}_3\text{O}_{12}$ can be prepared by the coprecipitation [10] and sol–gel [11–14] methods. The present paper describes the preparation of $\text{Bi}_4\text{Ti}_3\text{O}_{12}$ by the citrate and oxalate coprecipitation processes and subsequent calcination at high temperature. The role of pH, calcination temperature and time on the phase transformation are explained in relation to the experimental results.

2. Experimental

Oxalate coprecipitation [1,2] was modified for preparing the citrate and oxalate intermediates at different pH values (Fig. 1). With the subsequent calcination at 500–1000 °C for 1–4 h, the $\text{Bi}_4\text{Ti}_3\text{O}_{12}$ powder was obtained as determined by comparison with library spectra. The intermediates and the powder were then extensively analyzed and characterized.

3. Results and discussion

3.1. XRD

The XRD spectra of $\text{Bi}_4\text{Ti}_3\text{O}_{12}$ powder prepared from citrate and oxalate coprecipitation processes under different pH and temperature conditions are shown in Figs. 2 and 3.

The XRD spectra for the powder prepared at different pH values with the subsequent calcination at 800 °C (Fig. 2) show the $\text{Bi}_4\text{Ti}_3\text{O}_{12}$ phase containing $\text{Bi}_2\text{Ti}_2\text{O}_7$ and $\text{Bi}_{12}\text{TiO}_{20}$ as the impurities [15]. The best pH values that yielded the minimum content of the impurities for the citrate and oxalate processes were at 2 and 5, respectively. At the best pH values and the subsequent calcination at 500–1000 °C, the XRD spectra (Fig. 3) show that the

* Corresponding author.

E-mail addresses: ttphongtem@yahoo.com (T. Thongtem), somchaichiangmai@yahoo.com (S. Thongtem).

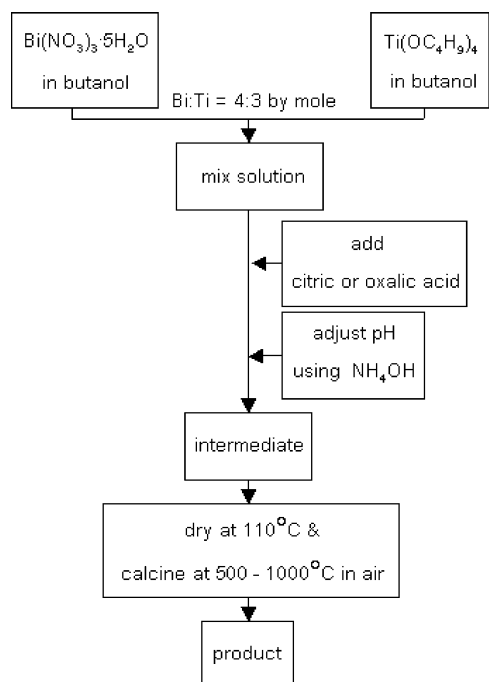


Fig. 1. Schematic diagram used for preparing citrate and oxalate intermediates and final product.

impurities were decreased with an increase in the calcination temperature, indicating that at high temperature the standard Gibbs free energies of formation of the impurities were increased as well. At 500 °C, the XRD peaks of the samples prepared from the citrate coprecipitation process were sharp indicating that the particles were crystalline in nature. But for the sample prepared from the oxalate coprecipitation process, the XRD peaks show the typical halo pattern indicating that the sample was amorphous. As the calcination temperatures were increased, the XRD peaks were sharper and the crystalline powder was obtained. The powder prepared from the citrate and oxalate coprecipitation processes and subsequent calcination at the temperature lower than 800 °C contains $\text{Bi}_2\text{Ti}_2\text{O}_7$ and $\text{Bi}_{12}\text{TiO}_{20}$ as the impurities. There was also spectral evidence for the precipitation of Bi_2O_3 from the citrate solution. At 800 °C and above, the $\text{Bi}_4\text{Ti}_3\text{O}_{12}$ phase contains very low concentration of the impurities. As the temperatures were increased, the impurities gradually decreased and purified $\text{Bi}_4\text{Ti}_3\text{O}_{12}$ was obtained at 1000 °C. At low temperatures, $\text{Bi}_4\text{Ti}_3\text{O}_{12}$ is in the tetragonal phase.

During the calcination, the crystal underwent the phase transformation from tetragonal to orthorhombic and the two structures were obtained. At 700 °C and above, the

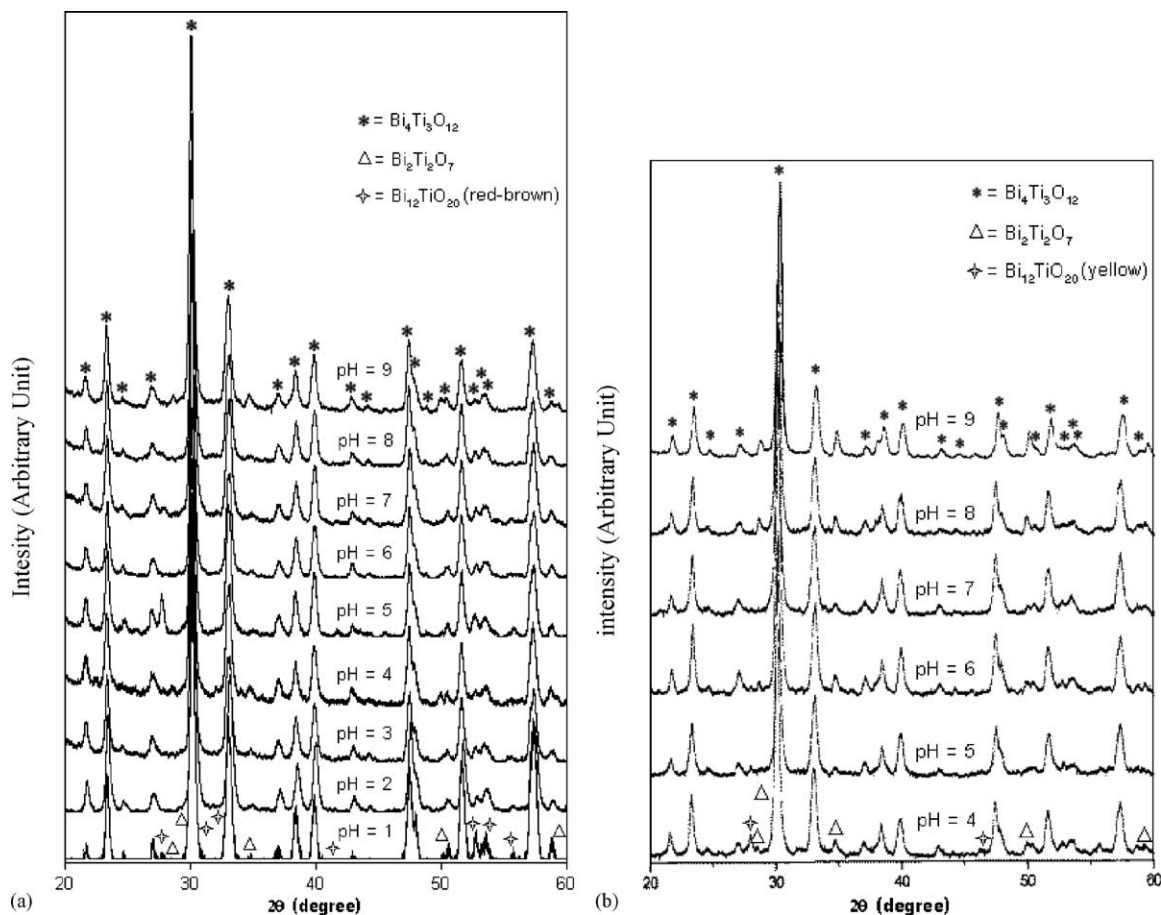


Fig. 2. XRD spectra of $\text{Bi}_4\text{Ti}_3\text{O}_{12}$ prepared from the (a) citrate and (b) oxalate coprecipitation at different pH values with the subsequent calcination at 800 °C for 1 h.

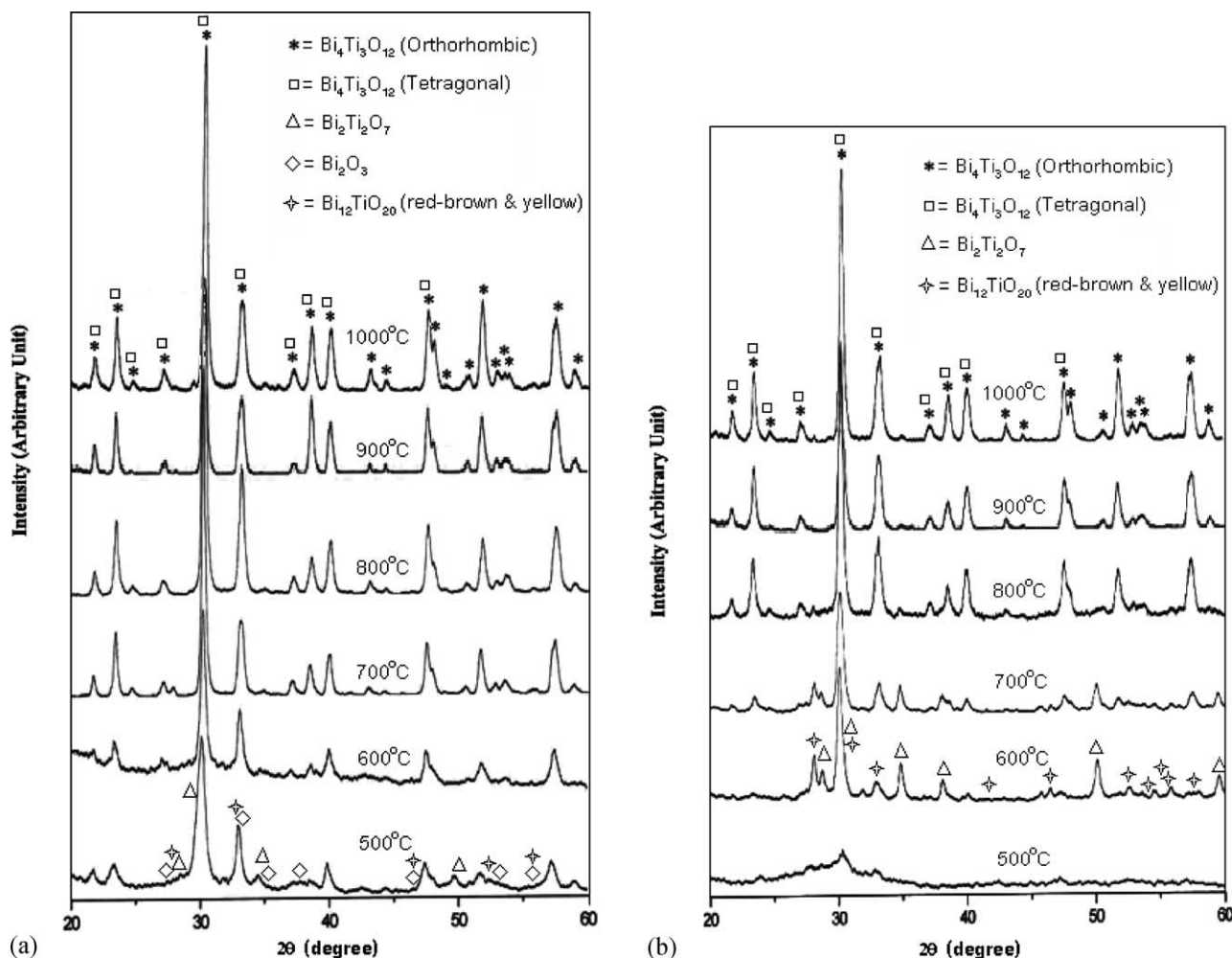


Fig. 3. XRD spectra of $\text{Bi}_4\text{Ti}_3\text{O}_{12}$ prepared from (a) citrate coprecipitation at pH of 2 and (b) oxalate coprecipitation at pH of 5 with the subsequent calcination at 500–1000 °C for 1 h.

orthorhombic structure become the dominant phase and was detected by the XRD. There are the differences between the angles and planes in the spectra that were used to identify the tetragonal and orthorhombic structures. The differences are shown in Table 1 [16,17]. The tetragonal structure consists of the two single peaks of (201)/(208) at 32.890°/39.655°, respectively. There were no splitting of the peaks at low temperature. As the temperature was

increased to 700 °C and above, the crystal underwent the phase transformation from tetragonal to orthorhombic. The peaks of (020)/(200), (028)/(208) and (137)/(317) were respectively detected at 32.853°/33.090°, 39.678°/39.880° and 56.928°/57.236°. Each pair of peaks is very close; therefore, the pair is virtually split. As the calcination time was prolonged to 4 h, there were no significant changes in the XRD patterns. It shows that the calcination time did not reflect the significant change of the impurity concentration.

Table 1

The selected 2θ and diffraction planes for the tetragonal and orthorhombic structures

Structures	2θ (°)	(hkl) Planes
Tetragonal	32.890	(201)
	39.655	(208)
Orthorhombic	32.853	(020)
	33.090	(200)
	39.678	(028)
	39.880	(208)
	56.928	(137)
	57.236	(317)

3.2. TGA

The thermal behavior of the precipitates obtained from $\text{Bi}(\text{NO}_3)_3 \cdot 5\text{H}_2\text{O}$ (A) and $\text{Bi}(\text{NO}_3)_3 \cdot 5\text{H}_2\text{O} + \text{Ti}(\text{OC}_4\text{H}_9)_4$ (B) in citric acid at pH of 2 is shown in Fig. 4(a). The A and B curves are very similar. They show the total weight loss of about 37–39%. At the temperature range 40–155 °C, the weight loss corresponds to the dehydration of water from the precipitate. At the temperature above the range, the main weight loss corresponds to the decomposition of citrate and other organic compounds. Due to the similarity of the A and

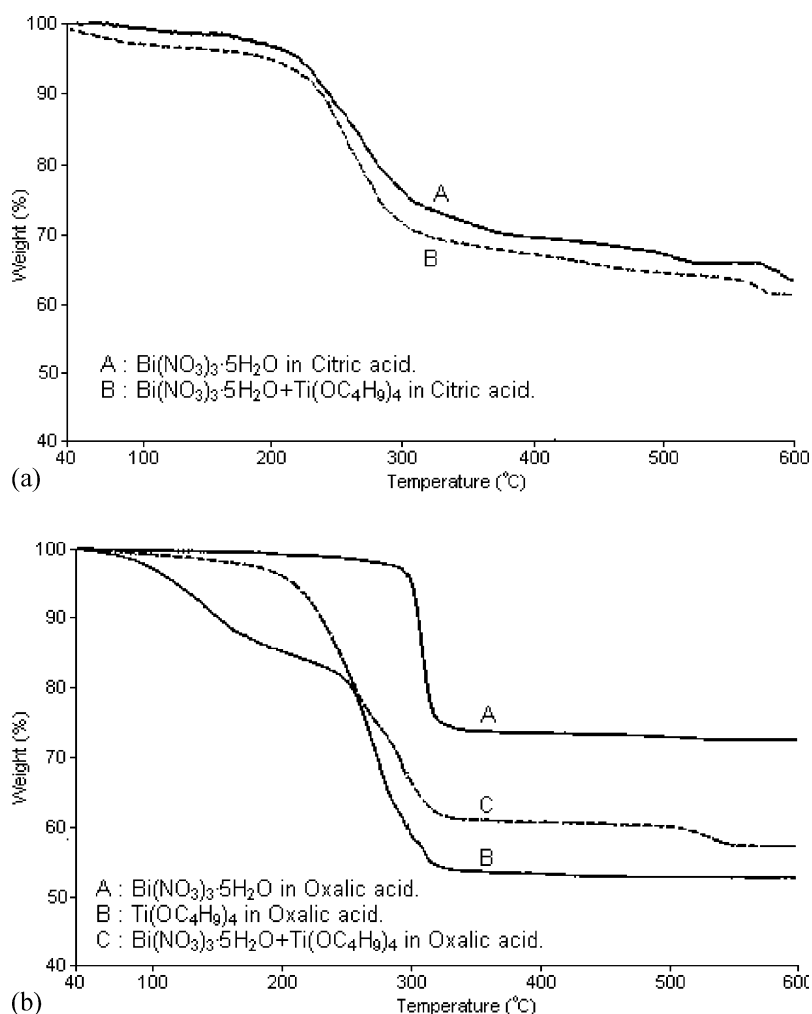


Fig. 4. The TG curves for the samples prepared from (a) citrate coprecipitation at pH of 2 and (b) oxalate coprecipitation at pH of 5.

B curves, both of the intermediates are the citrate salts in the solution containing citric acid.

The TG curves of the precipitates obtained from A = $\text{Bi}(\text{NO}_3)_3 \cdot 5\text{H}_2\text{O}$, B = $\text{Ti}(\text{OC}_4\text{H}_9)_4$ and C = $(\text{Bi}(\text{NO}_3)_3 \cdot 5\text{H}_2\text{O} + \text{Ti}(\text{OC}_4\text{H}_9)_4)$ in oxalic acid at pH of 5 are shown in Fig. 4(b). The A curve starts to show the weight loss at 246°C. The total weight loss is 25% and occurs in one step indicating the presence of bismuth oxalate in preference to bismuth hydroxide [3]. The B curve shows the total weight loss of 46.1%. The TG curve can be divided into two steps. The first weight loss of 16% corresponds to the dehydration of absorbing water and water from titanium hydroxide [3] at 40–212°C. The second weight loss of 30% corresponds to the decomposition of oxalate and the residual organic compounds (e.g., butanol) at 212–346°C. As the temperature is higher than 346°C, the curve is stationary. It shows that the precipitate consists of titanium hydroxide and titanium oxalate. The C curve resulting from the combination of the A and B curves shows the total weight loss of 42.5% over the temperature range 40–566°C. The first weight loss occurs by the dehydration of absorbing water and water from the ti-

tanium hydroxide intermediate. The second weight loss corresponds to the decomposition of bismuth–titanium oxalate and residual organic compounds. Most of the total weight loss is the result of the second one.

3.3. FTIR

The FTIR spectra of the intermediates and the calcined products prepared by the citrate and oxalate coprecipitation processes are shown in Fig. 5. In the vibrational spectra of the intermediates, peaks were detected in the 3300–3700 and 2600–3700 cm^{-1} for the citrate and oxalate precipitates, respectively. They could be the O–H stretching of the residual water and carboxylic acid. For the oxalate precipitates, the O–H stretching was also from the titanium hydroxide intermediate. Over the range 1690–1770 cm^{-1} , the modes are likely to be the vibration of C=O stretching bonds of carboxylic acids and/or the carboxylic derivatives. When the carboxylate groups formed bond with metal ions, the bands would shift accordingly by the replacement of the COO asymmetric stretching in the 1550–1650 cm^{-1} and

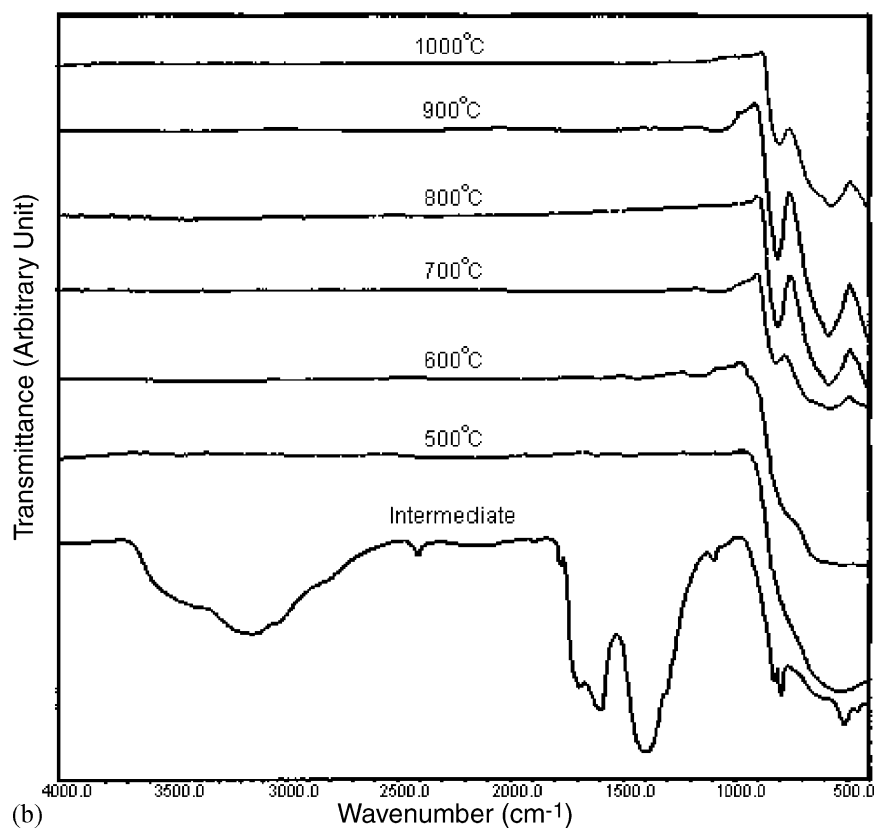
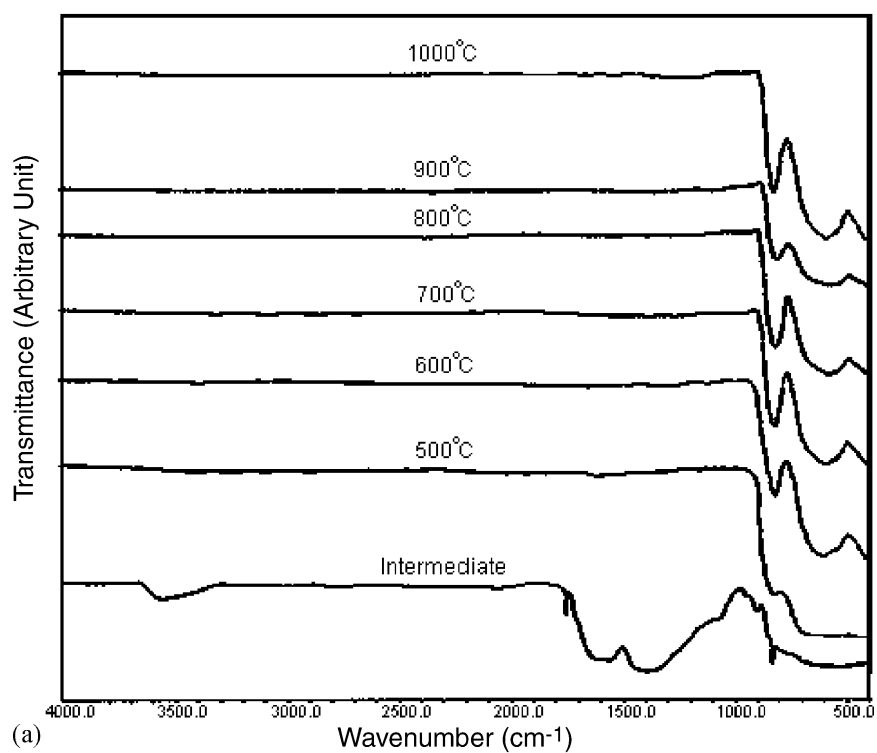


Fig. 5. FTIR spectra of $\text{Bi}_4\text{Ti}_3\text{O}_{12}$ prepared by (a) citrate coprecipitation at pH of 2 and (b) oxalate coprecipitation at pH of 5 with the subsequent calcination for 1 h.

COO symmetric stretching in the $1300\text{--}1450\text{ cm}^{-1}$. The formation of bonds between metals and oxygen from carboxylate groups results in peaks below 830 cm^{-1} [18].

When the intermediates were calcined at $500\text{--}1000^\circ\text{C}$, all the water and residual organic compounds were removed. The O–H, C=O and COO stretching bands disappeared. As the calcination temperature was increased, the bands of metal–oxygen bonds were gradually disclosed at 816 and 584 cm^{-1} for the powder prepared from citrate coprecipitation and at 811 and 574 cm^{-1} for the powder prepared from oxalate coprecipitation corresponding to the Ti–O stretching bands [4,19]. When the pH of the coprecipitation and the calcination time were varied, the vibrational spectra were also very similar to the previously described material.

3.4. SEM

The SEM micrographs of $\text{Bi}_4\text{Ti}_3\text{O}_{12}$ prepared from citrate and oxalate coprecipitation with the subsequent calcination at different temperature are shown in Fig. 6. At 500°C calcination, the samples prepared from citrate coprecipitation were crystalline powder with the particle size less than $1\text{ }\mu\text{m}$ but those prepared from oxalate coprecipitation contained an agglomeration of the particles. As the temperatures were increased, the degree of crystalline was improved. At 800°C and lower, the particle size gradually increased and the average particle size at 800°C was about $0.3\text{ }\mu\text{m}$. At the temperature higher than 800°C , the particle size was rapidly increased. The average particle size at 1000°C was about

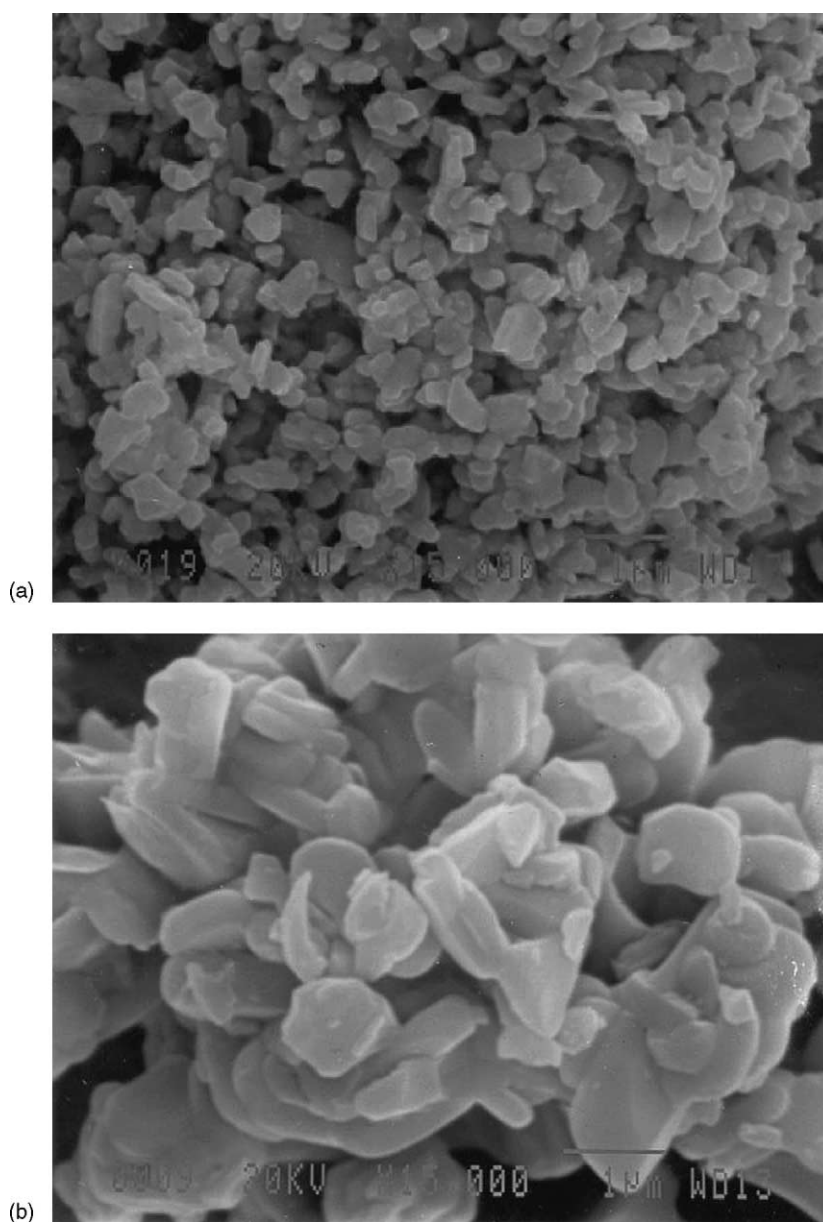


Fig. 6. SEM micrographs of $\text{Bi}_4\text{Ti}_3\text{O}_{12}$ prepared by citrate and oxalate coprecipitation and subsequent calcination for 1 h (a) citrate, 500°C ; (b) citrate, 1000°C ; (c) oxalate, 500°C and (d) oxalate, 1000°C .

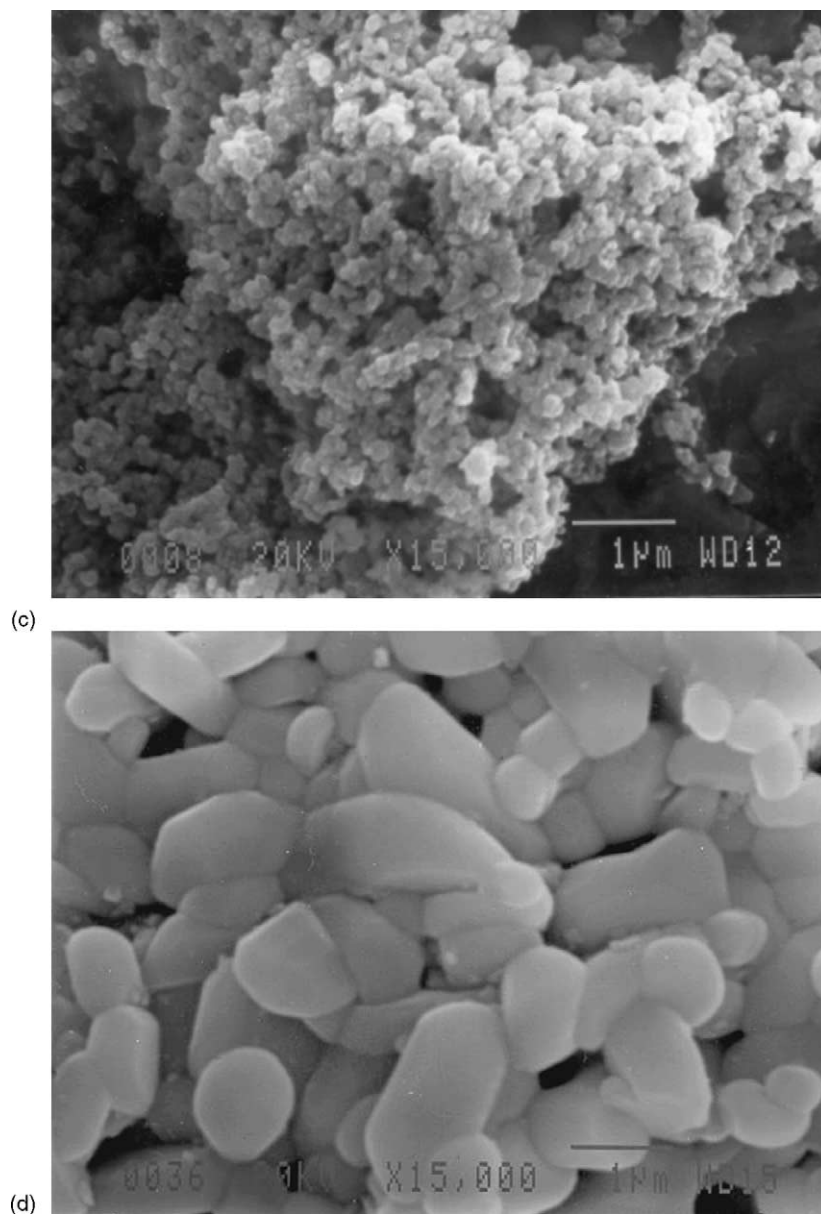


Fig. 6. (Continued).

1 μm . The results were consistent with the XRD spectra shown in Fig. 3.

4. Conclusions

Fine particles of $\text{Bi}_4\text{Ti}_3\text{O}_{12}$ were successfully prepared by coprecipitation of citrate at pH of 2 and oxalate at pH of 5 with the subsequent calcination at high temperature. The intermediates of the two processes were the citrate salt and oxalate–hydroxide mixtures which started to form the crystalline phases at 500 and 600 °C calcination, respectively. At 1000 °C, the average particle size from both intermediates was about 1 μm .

References

- [1] M. Villegas, C. Moure, J.F. Fernandez, P. Duran, *Ceram. Int.* 22 (1996) 15.
- [2] M. Villegas, C. Moure, J.F. Fernandez, P. Duran, *J. Mater. Sci.* 31 (1996) 949.
- [3] A.M. Umabala, M. Suresh, A.V. Prasadaraao, *Mater. Lett.* 44 (2000) 175.
- [4] Y. Kan, P. Wang, Y. Li, Y.B. Cheng, D. Yan, *Mater. Lett.* 56 (2002) 910.
- [5] Y. Du, J. Fang, M. Zhang, J. Hong, Z. Yin, Q. Zhang, *Mater. Lett.* 57 (2002) 802.
- [6] Y. Shi, C. Cao, S. Feng, *Mater. Lett.* 46 (2000) 270.
- [7] E.C. Subbarao, *J. Phys. Chem. Solids* 23 (1962) 665.
- [8] A. Fouskova, L.E. Cross, *J. Appl. Phys.* 41 (1970) 2834.
- [9] A.Q. Jiang, G.H. Li, L.D. Zhang, *J. Appl. Phys.* 83 (1998) 4878.

- [10] B.J. Mulder, Am. Ceram. Soc. Bull. 42 (1970) 990.
- [11] P.C. Joshi, A. Mansingh, M.N. Kamalasanan, S. Chandra, Appl. Phys. Lett. 59 (1991) 2390.
- [12] P.C. Joshi, S.B. Krupanidhi, J. Appl. Phys. 72 (1992) 5827.
- [13] N. Tohge, Y. Fukuda, T. Minami, Jpn. J. Appl. Phys. 31 (1992) 4016.
- [14] M. Toyoda, Y. Hamaji, K. Tomono, D.A. Payne, Jpn. J. Appl. Phys. 32 (1993) 4158.
- [15] Powder Diffraction File, International Centre for Diffraction Data, 12 Campus Bld., PA 19073-3273 (2001).
- [16] O. Yamaguchi, N. Maruyama, K. Hirota, Br. Ceram. Trans. J. 90 (1991) 111.
- [17] S. Cumins, L. Cross, J. Appl. Phys. 39 (1968) 2268.
- [18] K. Nakamoto, Infrared & Raman Spectra of Inorganic & Coordination Compound, Part B, fifth ed., Wiley, NY, 1997, p. 75.
- [19] D. Chen, X. Jiao, Mater. Res. Bull. 36 (2001) 355.